ONEIROS, a new miniature standalone device for recording sleep electrophysiology, physiology, temperatures and behavior in the lab and field

Bertrand Massot, Sébastien Arthaud, Baptiste Barrillot, Johanna Roux, Gianina Ungurean, Pierre-Hervé Luppi, Niels Rattenborg, Paul-Antoine Libourel

ONEIROS, a new miniature standalone device for recording sleep electrophysiology, physiology, temperatures and behavior in the lab and field.

Bertrand Massot [a], Sébastien Arthaud[b], Baptiste Barrillot[b], Johanna Roux[b], Gianina Ungurean [b, c], Pierre-Hervé Luppi[b], Niels C. Rattenborg[c], Paul-Antoine Libourel[b,#]

Corresponding author (Tel: +33 4 78 77 10 03; E-mail: pa.libourel@univ-lyon1.fr).

[a] INL, UMR5270 CNRS, INSA Lyon ; Université Claude Bernard Lyon 1; Villeurbanne, F-69621 ; France

[b] CRNL, SLEEP Team, UMR 5292 CNRS/U1028 INSERM; Université Claude Bernard Lyon 1; Lyon, F-69372; France

[c] Max Planck Institute for Ornithology, Avian Sleep Group, 82319 Seewiesen, Germany

ABSTRACT

Background: Sleep is an inactive state of reduced environmental awareness shared by all animals. When compared to wakefulness, sleep behavior is associated with changes in physiology and brain activity. The nature of these changes varies considerably across species, and therefore is a rich resource for gaining insight into the evolution and functions of sleep. A major obstacle to capitalizing on this resource is the lack of a small device capable of recording multiple biological parameters for extended periods of time both in the laboratory and the field.

New method: ONEIROS is a new tool designed for conducting sleep research on small, freely moving animals. The miniature, standalone system is capable of recording up to 26 electrophysiological signals (electroencephalogram, electromyogram, electrooculogram, electrocardiogram), metabolic (3 temperature channels) and behavior via an accelerometer for several days. In addition, the device is equipped with a vibrating motor which can be used to assess arousal thresholds and to disrupt sleep. The system is available in telemetric or datalogger configuration useable in the field.

Results: To demonstrate the efficacy of this tool, we simultaneously recorded for the first time, electroencephalogram, hippocampal local field potential, electromyogram, electrooculogram, brain, body and ambient temperature, and 3D accelerometry. We also deprived rats of paradoxical sleep by triggering the vibrating motor after online recognition of the state. Finally, by successfully recording a pigeon in an 8 m^3 aviary in a social context with the device in the logger configuration, we demonstrate the feasibility of using the device in the field.

HIGHLIGHTS:

- ONEIROS is a new miniature device with low power consumption dedicated to recording sleep

- The device can record sleep electrophysiology, physiology, and behavior in the lab or field
- An integrated vibrating motor can be used to assess arousal thresholds and perform selective paradoxical sleep deprivation

KEYWORDS:

Wireless, telemetry, datalogger, electrophysiology, sleep, pigeon, sleep deprivation

TABLE OF CONTENTS

I. INTRODUCTION

Sleep is a vital and complex behavioral state that competes with the time allocated to foraging, courtship, parental care, and vigilance (Lesku et al., 2012; Rattenborg et al., 2016, 1999). From a behavioral standpoint, sleep is traditionally defined as an inactive state with reduced responsiveness to environmental stimuli (i.e. elevated arousal threshold) that is rapidly reversible in response to sufficient stimulation. In many species, sleep occurs in a species-specific posture and at specific times of the day (Fig. 1.). The duration and intensity of sleep increases following sleep deprivation, indicating that it is homeostatically regulated (Campbell and Tobler, 1984; Piéron, 1913). Initially identified in mammals, two electrophysiological sleep states can be defined during behavioral sleep: paradoxical sleep (PS) or rapid eye movement sleep (REM sleep) and slow wave sleep (SWS) or non-REM sleep (NREM sleep) (Aserinsky and Kleitman, 1953; Jouvet et al., 1959). SWS is distinguished from wakefulness and PS by the presence of high amplitude, low frequency waves in the electroencephalogram (EEG), reduced heart and respiratory rate, reduced brain and body temperature, reduced muscle tone (compared to wakefulness), and the scarcity of eye movements. Environmental awareness is lower compare to resting wakefulness (Fig. 1.). During PS, the EEG exhibits a desynchronized (low-amplitude, high-frequency) wake-like pattern. In contrast to wakefulness, PS is associated with tonic skeletal muscle atonia (Jouvet et al., 1959). This atonia is phasically interrupted by rapid eye movements (Aserinsky and Kleitman, 1953) and other forms of muscular twitching, particularly in young mammals (Corner, 1977). In addition, heart and respiratory rates become irregular during PS (Snyder et al., 1964). Brain temperature increases, but all thermoregulatory mechanisms (i.e. muscle tone, pilo-erection, sweating, and shivering) are abolished (Jouvet et al., 1959; Parmeggiani, 2003). Finally, both SWS and PS are homeostatically regulated. Total sleep deprivation is compensated by an increase in the quantity and intensity of SWS (Borbély and Neuhaus, 1979), and selective PS deprivation is also followed by a recovery period with more PS (Dement, 1960).

	Quiet wake	Slow wave sleep	Paradoxical sleep	
Arousal theshold	-	+	+	Behavior
Homeostasis	-	+	+	
Specific posture	-	+	+	
Cortical EEG	Desynchronized	High amplitude slow waves	Desynchronized	Electrophysiology
Eye movements	+	-	+	
Muscle tone	-	-	--	
Muscle twitches	-	-	+	
Heart rate variability	+/-	-	+	Metabolism
Respiratory rate variability	+/-	-	+	
Body temperature	+	-	-	
Brain temperature	+	-	+	

Fig. 1. Table illustrating the main behavioral, electrophysiological and metabolic parameters that covary with the quiet states (Quiet wake, slow wave sleep and paradoxical sleep) in mammals.

Whereas it is largely accepted that sleep is present in animals ranging from jelly fish to the more complex animals (Campbell and Tobler, 1984; Nath et al., 2017; Omond et al., 2017; Raizen et al., 2008; Siegel, 2008), it is less clear whether all animals display two sleep states. Of the non-mammalian animals investigated, unequivocal evidence of mammalian-like SWS and PS was only found in birds (Dewasmes et al., 1985; Heller et al., 1983; Klein et al., 1964; Rattenborg et al., 2009). Nonetheless, some reports of a PS like state in non-avian reptiles (Libourel and Herrel, 2016; Shein-Idelson et al., 2016), or twitches during behavioral sleep in cuttlefishes (Frank et al., 2012) or in bees (Klein et al., 2008) suggest that two sleep states could also be present in other species.

Classically, sleep is studied in laboratory animal models (rats, mice, cats, dogs, fruitflies, and zebrafish) at various levels of analysis, including genetic, molecular, neuroanatomical, physiological, or cognitive. Several tools are available to assess these aspects of sleep; for example: optogenetic, immunohistochemical, behavioral tests, neuronal activity recordings, LFP, EEG, EMG, ECG, EOG, and temperature measurements. However, of the species in which sleep has been studied (less than 200 of the approximately 66 000 vertebrates), most of them were studied in to the lab via a tethered device that recorded EEG and EMG. A weakness of this approach is that using a tether could induce stress by reducing the animal's freedom of movement and precluding the use of sleeping shelters (Tang et al., 2004). Therefore, wireless alternatives are obviously required to reduce stress and foster more natural sleep patterns. Since 2000, one logger (Vyssotski, 2005; Vyssotski et al., 2009; http://www.vyssotski.ch/neurologger.html) and several telemetric systems with a limited transmission range (Lapray et al., 2008; Tang and Sanford, 2002; Weiergräber et al., 2005; Zayachkivsky et al., 2013) have been developed to record sleep-related EEG and EMG activity in rodents. The telemetry devices could record 1 or 2 channels at a low sampling rate (<1 kHz) for periods lasting from days to months, in the case of devices with

capacitive wireless transmission (Tang and Sanford, 2002). Other systems can record more channels (>32) at a higher sampling rate (>10kHz) needed to record neuronal activity (Harrison et al., 2011; Hawley et al., 2002; Mohseni et al., 2005; Sodagar et al., 2009; Yin et al., 2014). Nevertheless, with a battery of an acceptable size for a laboratory rodent to carry, these systems can only record for a few hours, which is insufficient for most sleep studies wherein disturbing the animals should be minimized. In general, it is essential that a sleep recording device records for at least 48 hours. Moreover, for comparative studies of species that do not exhibit sleep states readily comparable to mammalian SWS and/or PS based on EEG and EMG activity alone, it is important to record as many parameters as possible to facilitate comparison with mammals. Consequently, in the case of comparative sleep studies, behavioral, electrophysiological and metabolic parameters should be recorded in order to provide more informative features regarding how an animal sleeps. Unfortunately, none of the existing devices has enough channels to record multiple EEG, EMG, ECG and EOG channels, LFPs, and brain and body temperature for at least 48 hours, Moreover, none incorporates a means to evaluate the behavioral criteria of sleep, such as arousal threshold, reversibility, and homeostasis. Another important constraint is the weight and the size of the device. Obviously, all devices could record for a month with large batteries. However, most species are small and cannot carry heavy systems. Therefore, to increase autonomy, the power consumption of the system should be minimized.

In addition to these constraints, if the aim is to record the animal in the wild, other parameters are needed to describe sleep behavior. In the lab we often record video in conjunction with the electrophysiology, but in the wild, this cannot be done easily. An alternative is to record the animal's head movement with accelerometry along the three axes (Rattenborg et al., 2017). Moreover, as the quantity of sleep and the presence of topor/hibernation are temperature dependent, it is also important to record naturally occurring changes in ambient temperature in the wild. However, the major difference between recording in the lab and the wild is the manner in which the data is stored. In the lab, movement is usually restricted to a small space from which data can be transferred and stored on a computer via wireless transmission. However, in the field or in large enclosures (Lesku et al., 2011) that exceed the transmission range of small telemetry devices, the data needs to be logged on the device (Rutz and Hays, 2009). Currently, only one device available in various versions (http://www.vyssotski.ch/neurologger.html), is small enough, to record EEG and EMG combined with 3D accelerometry for sleep studies (Vyssotski, 2005). This device has been used successfully to record sleep-related electrophysiology and behavior in the field in sloths (Rattenborg et al., 2008; Voirin et al., 2014), sandpipers (Lesku et al., 2012), barn owl chicks (Scriba et al., 2013), and even frigatebirds in flight (Rattenborg et al., 2016). Although this device opened the door for the first field-based sleep studies and remains a powerful tool for many field-based sleep studies, the low number of channels (four) and the absence of a device for assessing arousal thresholds and disrupting sleep limits the scope of the questions that can be addressed with this device.

In summary, sleep is a universal and complex state, characterized by behavioral, electrophysiological and metabolic changes from wakefulness. Currently, multiple tools can assess some features of its phenotype in lab or more rarely in the wild, but none of them can measure the behavioral, electrophysiological, and metabolic features of sleep at the same time, in small species, for long periods. A device with these capabilities is needed for comparative and ecological experiments aimed at understanding the evolution and functions of sleep. Therefore, we developed ONEIROS (ONE Instrument for Recording Our Sleep), a telemetric/datalogger system

designed for sleep studies. This system is small enough to be worn by rats. The device can record 26 referential channels of electrophysiology (EEG, EMG, ECG, EOG or LFP), three temperature channels, and 3-axial accelerometry. Moreover, to evaluate the arousal threshold of to enforce sleep deprivation, the system includes a lightweight, vibrating motor. ONEIROS weighs less than 10g, when configured with a battery capable of recording for more than 48 hours. To validate the system, we simultaneously recorded for the first time the EEG, EMG, EOG, 6 LFPs in the hippocampus, the brain and body temperature, and 3D head acceleration of a rat. We also performed selective PS deprivation on a rat for 6 hours by activating the vibrating motor fixed on the device when PS was automatically detected via a custom online sleep scoring algorithm (Libourel et al., 2015). We compared the effect of the deprivation with published data obtained with gentle handling and automated deprivation methods. Finally, to demonstrate the feasibility of recording in the wild, we recorded a pigeon in a large aviary with other birds.

II. METHODS

1. Surgery and experimental recording conditions

1.1. Ethical considerations

All experiments were conducted with the 3R principles in animal experimentation and in accordance to the European Community Council Directive for the use of research animals (86/609/EEC and 2016/63/EU).

1.2. Rat baseline

Under ketamine-xylazine anaesthesia (100mg.kg^{-1} - 10mg.kg^{-1} respectively, I.P.), one Sprague Dawley male adult rat (230g, Charles River Laboratories, France) was placed on a stereotaxic frame (David Kopf Instruments, USA) and implanted for with sensors for recording the EEG, EMG, and EOG, as well as body and cerebral temperatures. Following incision of the scalp and removal of the skin, holes were drilled in the skull. EEG monitoring: two stainless steel screws (Bilaney, Plastics One, Germany) were fixed in the parietal (from bregma: anterior-posterior (AP), -4mm; medial-lateral (ML), +3mm) and frontal (AP, +3mm; ML, + 1mm) parts of the skull and two above the cerebellum (AP, -12mm; ML, +3mm) served as references. In addition, a 4-electrode bundle was placed in the hippocampus for LFP recordings. It was composed by 4-tungsten wires (35µm in diameter, Scientific Wire Company, England) with different lengths (500µm of difference for each). The bundle was inserted with the following coordinates: AP, - 3.8mm; ML, +1.8mm, and dorsal-ventral, -4mm, to record from the lower part of the dentate gyrus (longest wire) to the CA1 region (shortest wire) of the hippocampus. The screwscrews and bundle were fixed on the skull and electrically insulated from one another using acrylic Superbond (Sun Medical Co, Japan). EMG monitoring: two gold-coated electrodes were inserted into the neck muscles. EOG monitoring: two wires with gold-coated thin ball ends (1mm in diameter) were bilaterally placed under the eyelid, close to each eye. The wires were fixed on the skull with Superbond. Cerebral temperature monitoring: one additional hole was drilled in the occipital part of the skull and a thermistor (GA100K6MCD1, Measurement Specialties) was inserted close to the brain. The hole was filled with bone wax. Body temperature monitoring: one thermistor was inserted deeply between the neck muscles and secured with a suture. All wires were then connected to a head connector (Electronic Interface Board-36-PTB Neuralynx), which was secured to the skull using Superbond acrylic. Next, dental Paladur cement (Heraeus Kuzler) was applied around the head connector to protect all of the wires and the connector. At the end of the implantation procedure, the rat received

a non-steroidal anti-inflammatory injection (carprofene, 5mg.kg-1, S.C.) and was allowed to recover for 7 days, during which it was weighed and monitored daily. Then, the rat was housed in a Plexiglas barrel (30cm in diameter, Blox Usinage Plastique, France) with bedding, food and water *ad libitum* placed in a recording chamber with a 12h/12h light-dark cycle, ventilation, and a 23°C ambient temperature. ONEIROS was plugged into the animal's implant and baseline recordings started after 2 days' habituation to the device and the new environment. Signals were collected using DaqReverse, a custom Matlab (Mathworks, matlab r2016b) program, and were sampled at 256 Hz except for the temperature and accelerometer which were sampled at 64 Hz. Vigilance states were scored using SlipAnalysis a custom Matlab program with a 5-s sliding time frame window according to the following criteria: Active wake (AW) was characterized by desynchronized and irregular low-voltage and high-frequency (5-9 Hz) EEG activity, sustained EMG neck muscle tone, and movement detected by the accelerometer. EEG activity was similar during AW and Quiet wake (QW), but QW was differentiated from AW by the absence of movement. Slow-wave sleep (SWS) was characterized by high-voltage slow-waves (1.5-4 Hz) combined with low muscle tone similar to QW. Paradoxical sleep (PS) was characterized by a very regular theta rhythm (5-9 Hz) associated with muscle atonia (absence of muscle tone and accelerometer activity).

1.3. Rat Paradoxical Sleep deprivation

One Sprague Dawley adult rat (male, 270g) was used. The surgical procedure was the same as previously described. Briefly, four screws for EEGs were fixed on the skull bilaterally over parietal and frontal cortices and two screws over the cerebellum for references. Two EMG and two EOG electrodes, and brain and body thermistors were also implanted. At the end of the implantation procedure, the rat received a non-steroidal anti-inflammatory injection (carprofene, 5mg.kg-1, S.C.) and was allowed to recover for 7 days, during which it was weighed and monitored daily. The rat was first placed in the recording chamber for baseline recording. Data were sampled at 128 Hz except for temperature and accelerometry which were sampled at 64 Hz. The baseline signals were scored and template parameters for each state were extracted from the EEG and EMG for online sleep scoring (Libourel et al., 2015). To enforce PS deprivation (PSD), we used an online algorithm to detect PS (Libourel et al., 2015) and a vibrating motor embedded on the ONEIROS device (Fig. 2. A) to awaken the rat when PS was detected. The vibration intensity was set to 100% and the stimulation duration was 700 ms. After a 6-h period of PSD, the rat was recorded for an additional 6-h recovery (PS recovery - PSR). The time spent in each vigilance state was quantified during baseline, PSD, and PSR.

1.4. Pigeon baseline

One adult pigeon (one female, *Columbia livia*, 250 g) was anesthetized using isoflurane, then placed in stereotactic device (David Kopf Instruments, USA) and instrumented for EEG, EMG, EOG recordings. For EEG monitoring, four gold-plated, round-tipped (0.5 mm diameter) electrodes (Bürklin, Germany) were placed over the anterior and posterior hyperpallium (Wulst), a primary visual area. The electrodes were symmetrically placed, 4 mm apart along the AP axis and 2.5 mm and 3 mm from the midline for the anterior and posterior electrodes, respectively. Two electrodes were placed above the left and right sides of the cerebellum served as references for the ipsilateral EEG electrodes. For EOG monitoring, two electrodes were

placed in the porous bone cavity behind the top of the eye; the electrodes did not enter the orbit. After positioning, the EEG and EOG electrodes were secured with dental acrylic. For EMG monitoring, two wire electrodes were inserted into the nuchal neck muscles. To ensure a good adhesion between the dental acrylic and the bone, small holes were drilled through the top layer of the cranium, which allowed the acrylic to infiltrate the bone. The electrodes, cables and the connector were embedded in dental acrylic. At the end of the implantation procedure, the bird received an intramuscular injection of meloxicam (Metacam 2mg/kg) for post-operatory analgesia. The pigeon was allowed to recover for 24 hours before attaching the data transmitter to the connector on its head. For the recordings, the device was equipped with a 1 Gb SD card and was attached to the connector on the bird's head. The pigeon was then placed in an all-female group aviary (2 m x 2 m x 2 m) together with another three uninstrumented birds. The aviary was equipped with an infrared camera for video monitoring (Axis M20 Network Camera Series). The EEG, EMG, EOG and 3-axis accelerometry were recorded in logger mode at 256 Hz for 24 hours. At the end of the recordings, the bird was recaptured, the device was removed and the data collected from the SD card. All animals had *ad libitum* access to food and water. The aviary had a 12h/12h light-dark cycle and an ambient temperature of 20°C.

2. A new device to quantify sleep

2.1. Embedded system for data acquisition

ONEIROS was designed to provide a flexible set of tools, fitting in a tiny device, for the analysis of sleep in small animals. It includes an integrated, low-power electrophysiology frontend to measure up to 26 biosignals, 3 temperature signals, and 3 accelerometer axes. An additional vibrating motor can be connected to the system and controlled using either real-time or predefined sequences of variable durations and intensities of vibration to assess arousal thresholds or prevent sleep. The system can be used either as a data logger, by using an embedded media storage, or as a telemetry device for real-time monitoring and analysis of the signals. The overall hardware architecture and software embedded on the system were developed to ensure that it would match the requirements (number of channels needed and bandwidth) of various possible experimental conditions and animal species. The size of the entire electronic system is 9 mm x 16 mm x 25 mm and it weighs 4 g. Together with a small 3 Volts, 150 mAh Li/MnO2 primary battery of 1.4 g (CP251525, GMB Company Ltd.) it can be encapsulated in a 28 mm x 18 mm x 15 mm plastic enclosure (Fig. 2. B). The addition of the vibration motor requires an additional width of 2 mm on one side of the enclosure and a weight of 1 g.

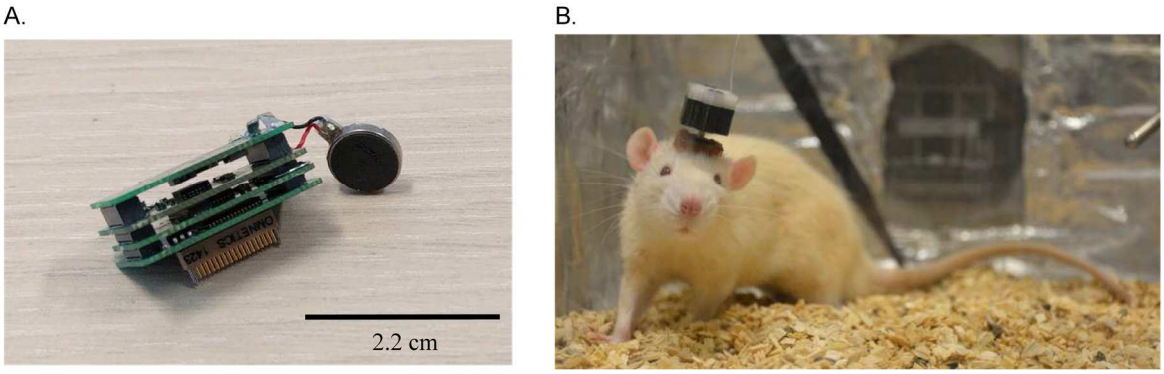

Fig. 2. A. Picture of the device showing the stack of boards with circular vibrating motor connected. B. Picture of a rat with the enclosed wireless device on its head.

2.2. Hardware boards

To enable rapid changes and optimizations of the main system functions, we designed small printed circuit boards which can be stacked together to form a functional measurement system (Fig. 2. A). The boards are interchangeable allowing adaptation of the system to specific experiment conditions. This modularity also allows for future improvements of the main functions. In the current version, four boards form a fully working system: a power stage, which provides independent power from the battery for the analog and digital boards; a communication stage which consists of either an embedded memory storage board, or a wireless data transfer board; an analog stage which contains the frontend for the acquisition of biosignals; and, finally, a digital stage which controls and synchronizes data acquisition from the analog stage and transfer to the communication stage. The connection between each stage is made by stackable connectors on a single side or on both side of the board depending on the position of the board in the system (for example, the power board contains connectors only on the bottom side as it is the upper stage of the system). The global interconnection between all boards is shown on Fig. 3. Any board can be replaced by any other one of the same type, as long as the connectors' placement and pinout is retained. To minimize noise on the analog signals, the analog power supply and the serial bus to the analog frontend are placed on the first stack of connectors. The digital power supply, control lines and serial bus to the digital boards are placed on the second stack of connectors at the opposite of the circuit board. The overall functional diagram of the current version of the system is shown on Fig. 3.

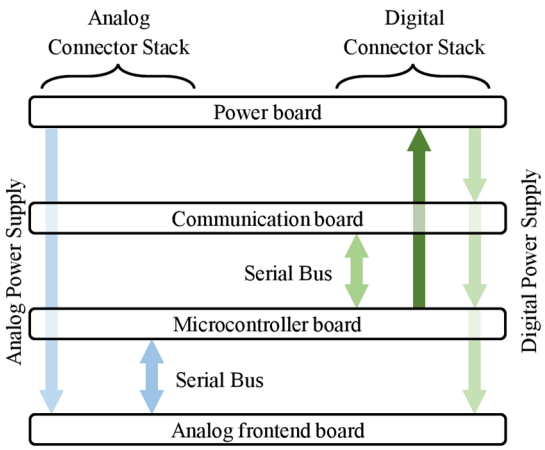

Fig. 3. Diagram of the interconnection between hardware modules

2.3. Power board

The power board is placed at the top of the system stack, together with the battery. The electronic circuit is mainly composed of a dual channel boost-converter (LTC3535, Linear Technology Corporation) to provide constant voltages for analog and digital power supplies from the voltage of the battery, which can vary from 3.2 V down to 2 V at the end of the battery life. Due to the voltages required by the communication and analog frontend stages, the boost-converter is configured to output 3.3 V for the digital power supply with up to 100 mA output current (required in case of the use of a micro-SD card in the communication stage). On the other hand, the second channel of the boost-converter is configured to output 3.6 V for the analog power supply, which is subsequently fed into a 3.3 V low-noise, low-dropout regulator (LDO). The dedicated LDO (LP5907, Texas Instruments Inc.) is used to minimize the output ripple of the boost-converter on the analog power supply, as the amplifier stage of the analog frontend board can be very sensitive to power supply variations and noise. The power board also contains a light indicator (low power LED) connected to the digital connector stack and can be controlled by the microcontroller and used to indicate the state of the device. The power switch is a Hall Effect, bidirectional latch (AN48846B-NL, Panasonic Corporation) which can be opened and closed using a proximity magnet. This enables control of the power board even when the system is enclosed in a waterproof housing.

2.4. Communication board

Two communication boards have been developed and can be exchanged depending on the environmental conditions of the measurement as well as the requirements of the experiment. The first board is composed of a micro-SD card interface, and enables the embedded recording of acquired data on a memory card. With this board, the system is used as an autonomous data-logger system mounted on the animal; the data is retrieved from the memory card after the experiment. The second board developed is composed of a 2.4 GHz transceiver (nRF24L01p, Nordic Semiconductors) and an associated radio-frequency (RF) circuit and ceramic chip antenna. When assembled with the RF communication board, the system is used as a wireless telemetry system and the data are collected in real-time by using a base-station receiver connected to a computer via a Universal Serial Bus (USB) cable. As described, the modularity of the system enables it to record in laboratory conditions, with real-time acquisition of the data, as well as in a natural or semi-natural environment where the animal can freely move with the device in the data-logger configuration.

2.5. Analog frontend board

The analog frontend board is intended to be placed at the lower stage of the board stack, as the connector (Omnetics, Dual Row Nano Strip series, 32 contacts) is located on the bottom side of the board for linking the electronic interface board (EIB) to the electrodes and temperature sensors on the animal. The board is based on the RHD2132 (Intan Technologies, LLC.) digital electrophysiology interface chip. This low-power, integrated circuit contains a 16-bit analog/digital converter (ADC), a 32 channels low-noise amplifier with programmable bandwidths and 3 additional auxiliary inputs. The 3 auxiliary channels are used for temperature measurements with negative-temperature coefficient thermistors of 100 kOhm at 25 °C. Due to hardware (EIB connector) and software limitations, only 26 amplified channels are used for electrophysiology measurements which make a total of 32 channels when combined with temperature (3 channels) and three accelerometer axes. Data acquisition is triggered independently for each channel, and the ADC result is retrieved using the serial

communication bus connected to the micro-controller board. This enables each channel to be independently sampled at different rates as described in the software section. This flexibility allows the user to adjust the power consumption of the device through changing the sampling rate required for each biosignal, temperature, and accelerometer axis.

2.6. Microcontroller board

The microcontroller board contains the microcontroller unit (MCU) and the digital accelerometer integrated chip, as well as a driver for the vibrating motor. The accelerometer is an ADXL362 (Analog devices, Inc.), a 3-axis MEMS accelerometer with a resolution of 12 bit and an average active consumption of 2 µA. The microcontroller used in the system is a MSP430FR5969 (Texas Instrument, Inc.). This microcontroller was selected due to its very low-power consumption of 100 µA/MHz and its flexibility in terms of power management (1 active and 3 low-power modes of operation). The software embedded on the microcontroller is described in the section 2.7. The microcontroller is connected to three communication serial buses using the Serial Protocol Interface (SPI) to control and transfer data from the accelerometer, the analog frontend board, and the communication board. Additionally, the microcontroller is directly connected to a universal haptic drive (DRV2603, Texas Instruments Corporation) which controls an 80 mA vibration motor that can be connected directly to the microcontroller board.

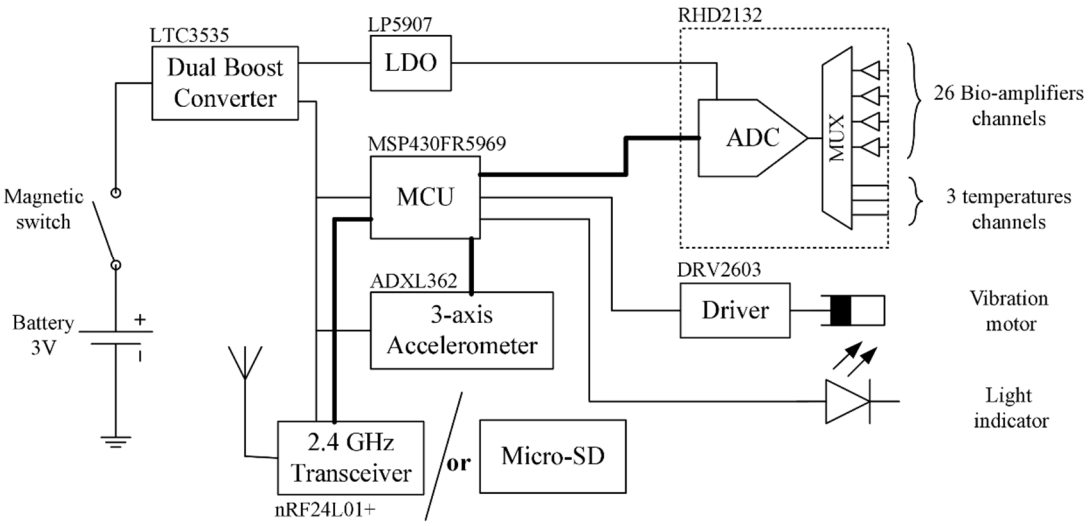

Fig. 4. Functional diagram of the complete instrumentation

2.7. Software embedded on the microcontroller

The software embedded on the microcontroller was developed using the Code Composer Studio integrated development environment (Texas Instrument, Inc.). The software was written in C language, compiled using the TI compiler and transferred to the microcontroller with an EZ-FET programmer for the MSP430 microcontroller family. The role of this software is to provide flexibility and adaptability of the instrumentation to the specific needs of each experiment (i.e. the number of channels used among the 32 channels available, and a dedicated sampling frequency for each individual channel). As a result, this method of acquisition has the advantage of

minimizing the power consumption of the entire system when less channels or lower sampling rates are required, thus extending the autonomy of the device for longer experiments.

At startup, the first task of the software is to detect whether the telemetry or the logger board is used for recording data and to configure the peripherals accordingly. Then the program enters an infinite loop where three different states are executed sequentially: a) retrieving the sampling rate of each channel, b) generating an acquisition sequence based on the table of sampling frequencies, and then c) indefinitely acquiring and transferring samples (following the generated sequence) until the system is stopped by power down or configuration change. If using a telemetry configuration, where data are transmitted to a remote computer, the software is able to receive real-time orders to control the vibration motor. In that case, an algorithm executed on the remote computer can automatically use the data received from the system to, for example, classify awake or sleep states of the animal and then send back vibration commands to induce sleep deprivation or to assess arousal threshold. Fig. 5. illustrates the overall execution of the program with annotations regarding telemetric or logger specific usages.

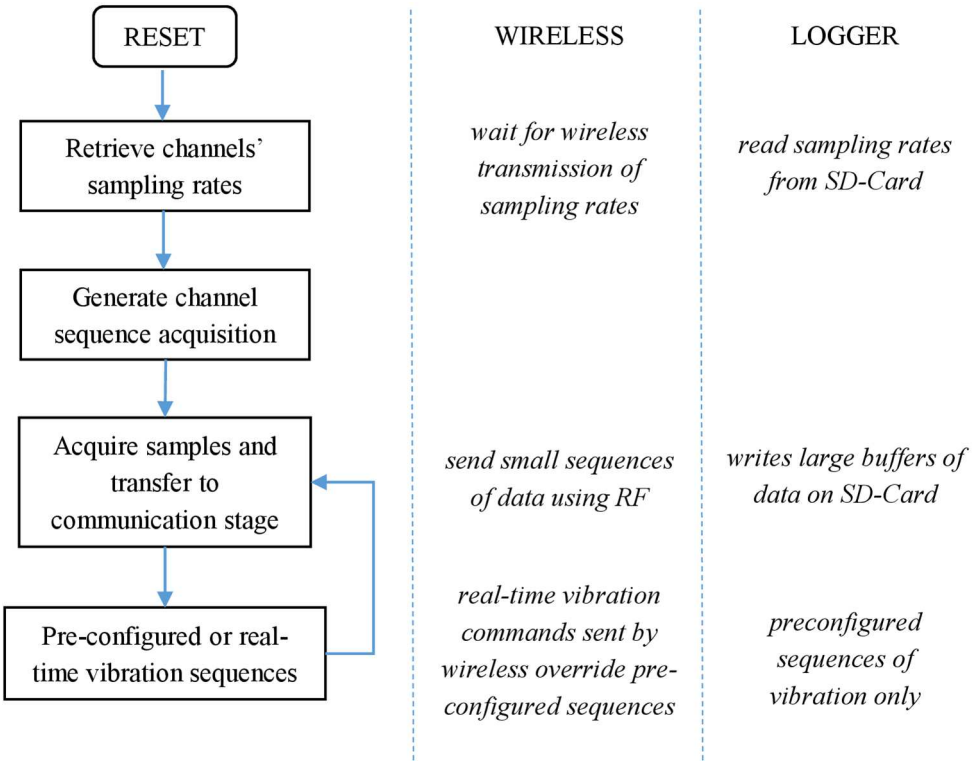

Fig. 5. Flowchart of the embedded software on the micro-controller unit

2.8. Signals description and acquisition

The device enables the acquisition of 32 different channels of three different types: a) 26 channels for biosignals, including a reference channel, b) 3 channels for temperature based on negative temperature coefficient (NTC) thermistors, c) 3 channels for accelerometry based on a 3-axis digital accelerometer. Due to limited wireless bandwidth, and also to limited power consumption when using the logger configuration, the overall maximum sampling frequency is set to 8192 samples per second (sps). This maximum sampling rate can be split over the different channels via software (Fig. 6.) in any combination as long as the sum of all

frequencies is equal to or lower than 8192 Hz (for example, 1 channel sampled at 8192 sps or 8 channels sampled at 1024 sps). Based on the sampling rate defined for each channel individually, the embedded software automatically generates a sequence of acquisition at a fixed clock rate with respect to every channel frequencies. For timing precision, a 32.768 kHz crystal oscillator is used with a drift of only 20 ppm or less. Then every possible sampling frequency that is an integer divisor of this clock (8192, 4096, 2048, 1024, etc.) can be set. When sent using wireless communication, data are collected using a RF remote receiver connected to a remote computer using a USB connection. The remote receiver is composed of the same transceiver chip (nRF24L01p) as the transmitter, and is associated to a PSoC 5LP (Cypress Semiconductors) microcontroller unit which transmits sampling rate configurations to the system and collects data frames which are subsequently sent to the computer through USB port. On the host computer, a dedicated driver as well as graphic user interface have been developed using Matlab (The Mathworks) to facilitate configuration, real-time visualization and control, as well as storage of the data (Fig. 6.).

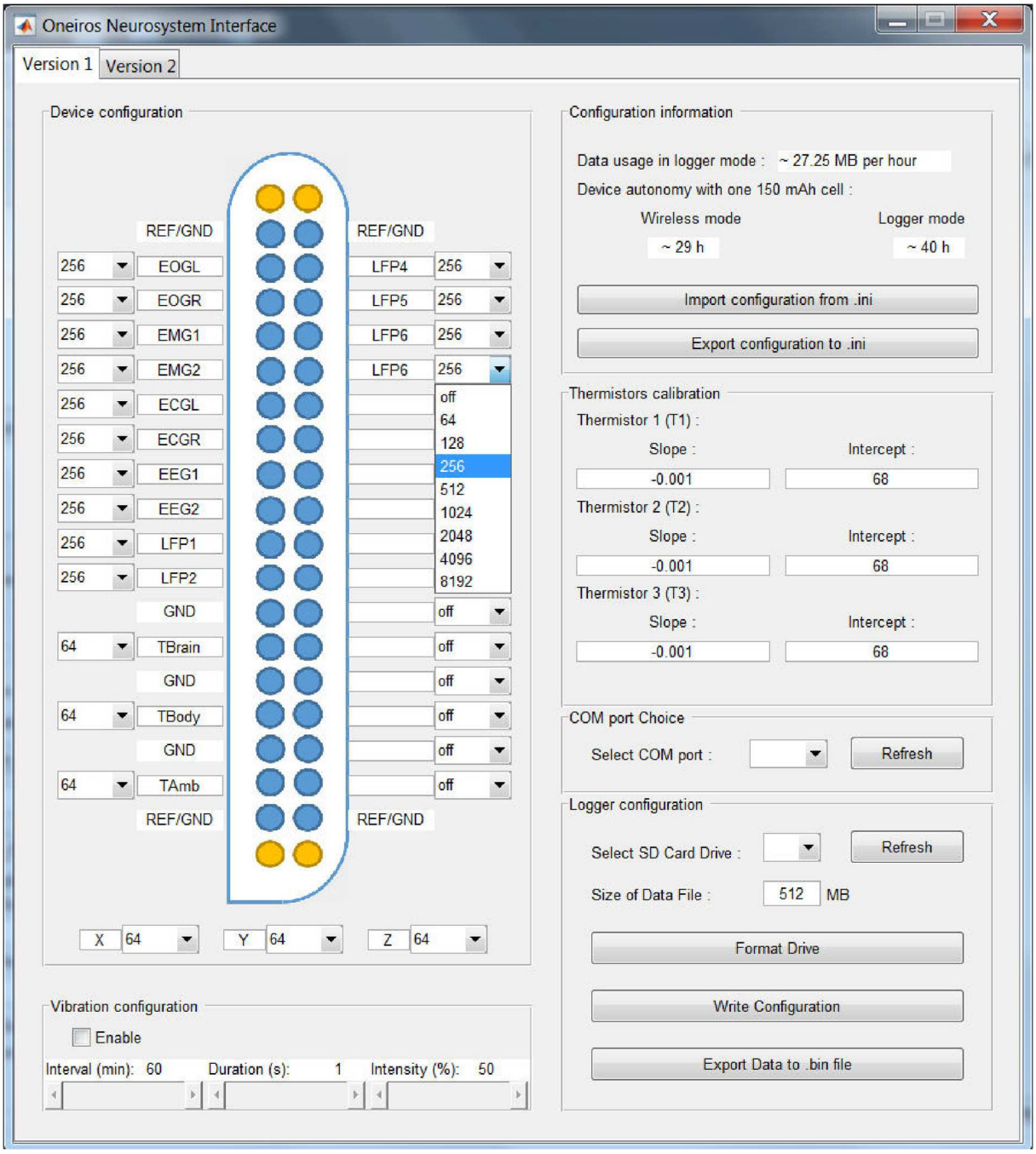

Fig. 6. Screen shot of the configuration tool design on Matlab for allocating the sampling rates to the different channels.

2.9. Biosignals

The 26 unipolar channels for biosignal measurements are acquired through the analog frontend which contains one instrument amplifier (referred to a reference electrode) for each channel with a fixed gain of 192 V/V. The output of all amplifiers can be multiplexed to the input of a single 16-bit analog to digital converter. These channels are meant to measure biosignals, such as EEG, ECG, EMG, EOG and LFP. Each channel has a

digital precision of 0.195 µV and total voltage range of +/- 6.39 mV. Integrated and configurable analog bandpass filters prevent aliasing effects and enable DC removal.

2.10. Temperatures

The analog frontend contains three auxiliary (not amplified) analog channels used to acquire temperature measured with NTC, 100kOhm thermistors. The thermistors (GA100K6MCD1, Measurement Specialties) are polarized with voltage from a voltage divider by using a 100kOhm resistor (Fig. 7.). Auxiliary inputs are sampled through the same analog to digital converter as the biosignals, but with a voltage range of 0 – 2.4V. When using the voltage divider to polarize the thermistor, the linearity error is lower than 1% in the range 15 – 40°C, and variations lower than 0.002 °C can be measured.

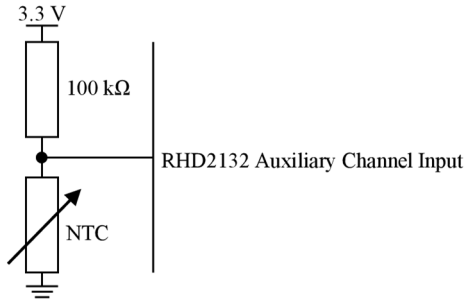

Fig. 7. Temperature measurement circuit diagram

2.11. Accelerometry

A 3-axis, 12-bit digital accelerometer is used to assess movement of the animal's head. By using a range of +/- 1g, the accuracy of the measurement is 0.001g. Internal bandwidth can be configured depending on the sampling frequency to avoid aliasing. Data are directly retrieved by the microcontroller through a serial peripheral interface (SPI).

2.12. Electrical characteristics

Although analog signal processing, analog to digital conversion, and digital interfaces with the microcontroller contribute to the overall power consumption of the system, for the most part, the autonomy of the system will depend on the communication board. Whether it uses RF communication or SD-Card storage, this stage has much higher power consumption when handling data. Hence, its consumption depends on the amount of data collected by the system; i.e. the total sampling rate of the configuration. In order to predict the autonomy of the system, the overall consumption has been accurately measured for different sampling frequencies (Fig. 8.).

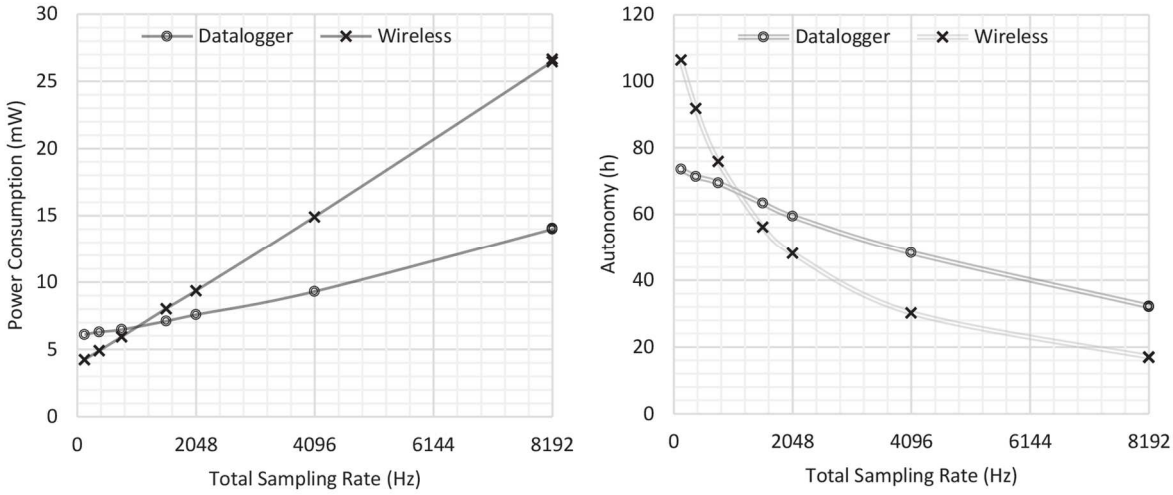

Fig. 8. Power consumption of the system with a 3V supply voltage and expected autonomy with a 150mAh primary battery.

III. Results

1. Multiple parameters recorded in baseline condition with ONEIROS (telemetric version) in a rat

To validate the design of our system (size, weight, signal quality, and autonomy), we first monitored a rat in standard lab conditions. Here, for the first time we were able to record at the same time most of the electrophysiological parameters that covary with the different states of vigilance. Fig. 9. A. illustrates 90s of raw signal recorded with ONEIROS and Fig. 9. B. shows 10s of each state. The characteristics and quantity of each state were consistent with previously published data (Fig. 10.). During active wake (AW: dark blue), EEG and hippocampal activity is desynchronized, with the later also showing a sustained theta frequency (around 6Hz, see time frequency plot) characteristic of periods of locomotion (see also Fig. 9. and Fig. 10. D.) (Sławińska and Kasicki, 1998). The EMG, EOG, and the accelerometer show bursts of intense activity. The brain and nuchal temperature are at high levels. During QW (light blue), the animal stops moving, as reflected in the EMG and accelerometry recordings. Eye movements become less frequent and the EEG tends to increase in amplitude and decrease in frequency when compared to AW (Fig. 10. B). During SWS (red), the EEG is dominated by large slow waves (Fig. 9. and Fig. 10. D). During SWS, the EMG remains at a low level, the accelerometry shows little variation, indicating the absence of movement, and eye movements are nearly absent. Both temperatures tend to decrease during SWS. When the animal falls into PS (green), the parietal EEG and hippocampal recording show typical activity in the theta band (Fig. 9. and Fig. 10. D), eye movements occur, the EMG becomes atonic, the brain temperature increases to wake levels, but body (nuchal) temperature continues to decline (Fig. 9., Fig. 10. C). A small nuchal “twitch” is also visible on the accelerometer signal (Fig. 9. B). Although high voltage waves were observed when the animal knocked the device against the cage wall, the signals were usually free of artefacts, even during grooming and locomotion.

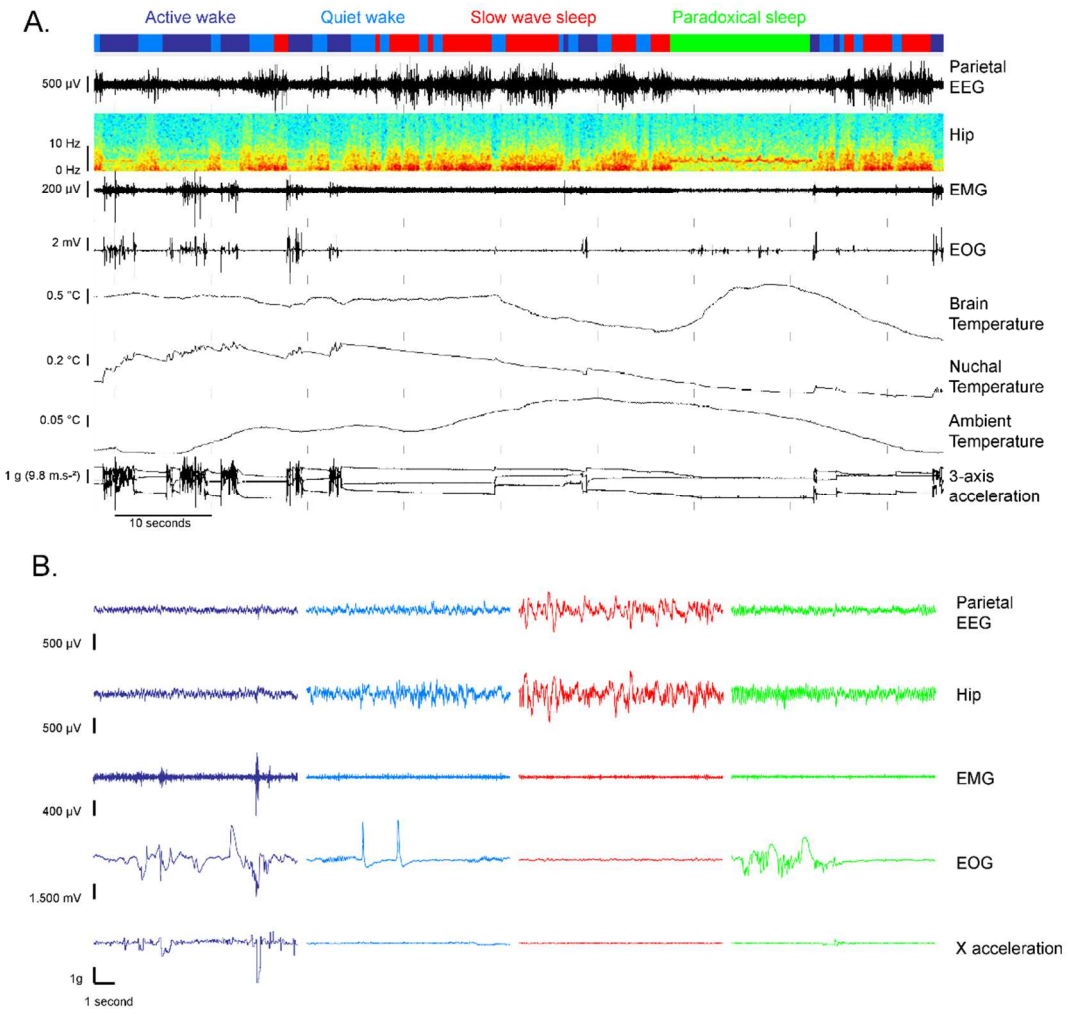

442

443

444 **Fig. 9.** Raw signals obtained with ONEIROS in telemetric mode from a rat during different vigilant states. A.
445 90 second recording of all signals. From the top to the bottom; hypnogram illustrating the wake/sleep scoring
446 (active wake in dark blue, quiet wake in light blue, slow wave sleep in red, and paradoxical sleep in green);
447 parietal EEG; time frequency representation of the hippocampal local field potential (color coded from -131 dB
448 in blue to -73 dB in red); EMG with a high pass filter (cutoff frequency 10Hz, order 2); EOG; brain temperature;
449 nuchal temperature; ambient temperature; 3 axial accelerometry. B. Representative 10 second examples of the
450 parietal EEG, hippocampal LFP, EMG, EOG and acceleration along x axis, occurring during the four states.

451

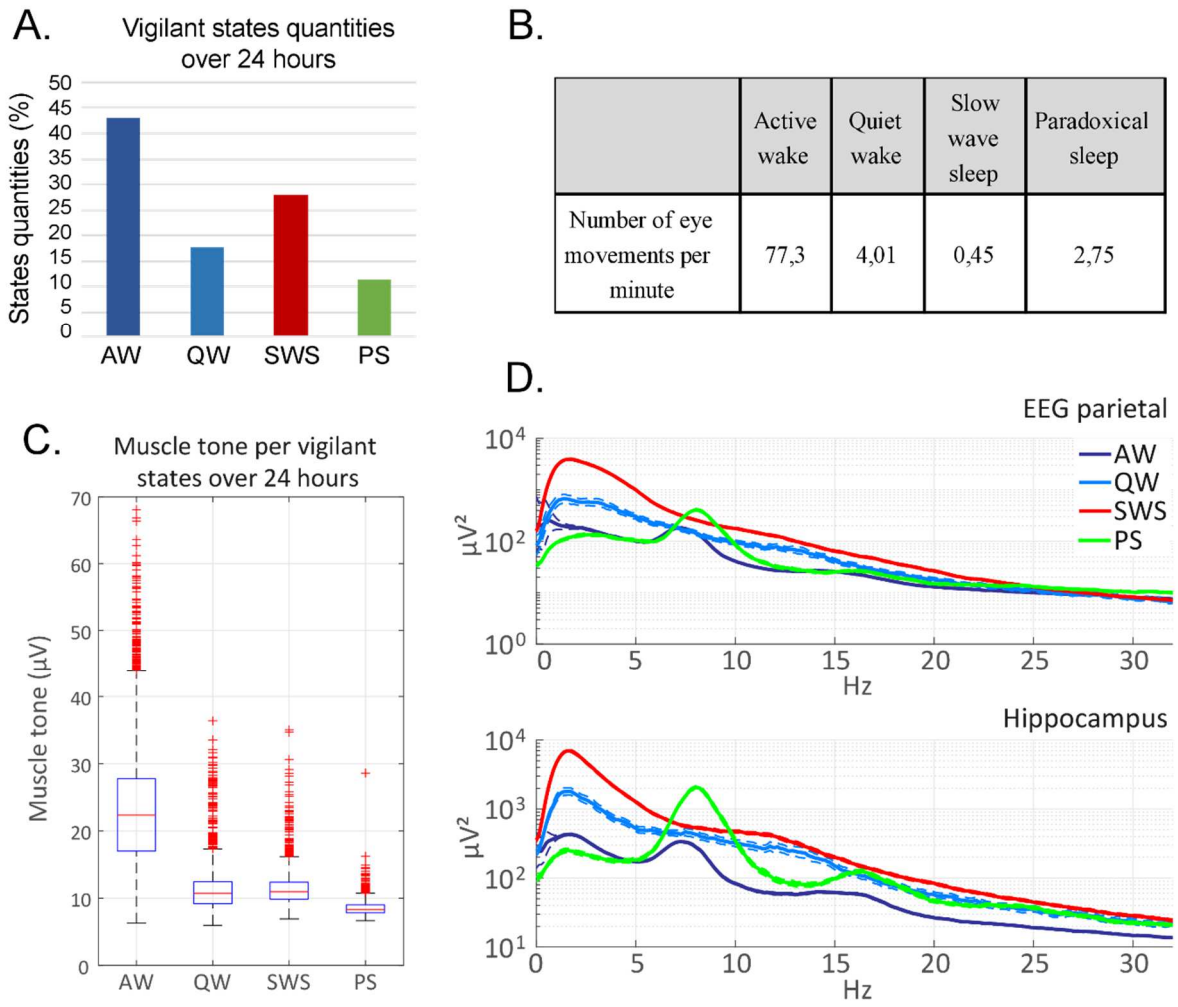

	Active wake	Quiet wake	Slow wave sleep	Paradoxical sleep
Number of eye movements per minute	77,3	4,01	0,45	2,75

Fig. 10. Results over 24 hours obtained from telemetric recordings in a rat. A. Quantification of the vigilant states over 24 hours. B. Number of eye movements per minute per state. C. Distribution of the muscle tone per epoch for each state. D. Power spectrum in each state computed for the parietal EEG and hippocampal LFP.

2. Selective paradoxical sleep deprivation in a rat using ONEIROS

The vibrating motor embedded in the ONEIROS device (Fig. 2. A.) was used to evaluate its efficacy in suppressing PS for several hours and inducing a homeostatic increase in PS during post-deprivation recovery. We performed selective PS deprivation for 6 hours by using a probabilistic online sleep scoring algorithm (Libourel et al., 2015). Fig. 11. illustrates the raw signals during the PS deprivation (PSD) experiment (see also supplementary video 1). After a few seconds of PS (see atonia and EEG desynchronization), the algorithm sends a stimulation (white bar on the bottom bar) that immediately awakens the animal (supplementary video 1). The latency to detect PS was around 3-4 seconds. Fig. 11. B. shows the percentage of PS per hour during and after the deprivation (in green) compared to baseline conditions (in blue). The deprivation reduced the quantity of PS for 6 hours by 60% (58% in baseline to 23% during PSD). Moreover, PSD also induced a rebound of PS (PSR) quantity during the recovery period with an increase of 85% over baseline levels (14% in baseline vs 26% during

PSR, Fig. 11. D.). Compared to 4 hours of PSD via gentle handling (Ravassard et al., 2016), Fig. 11. E) and unpublished data from our lab using a mechanical shaking device (Viewpoint S.A., (Libourel et al., 2015), the quantity of remaining PS during PSD with ONEIROS is higher (5% with ONEIROS compared to 2.6% and 2.7% with the other methods). This is due to the presence of PS episodes during which the stimulations didn't immediately awaken the animal. However, PS quantities during the recovery were consistent with those obtained with the other methods.

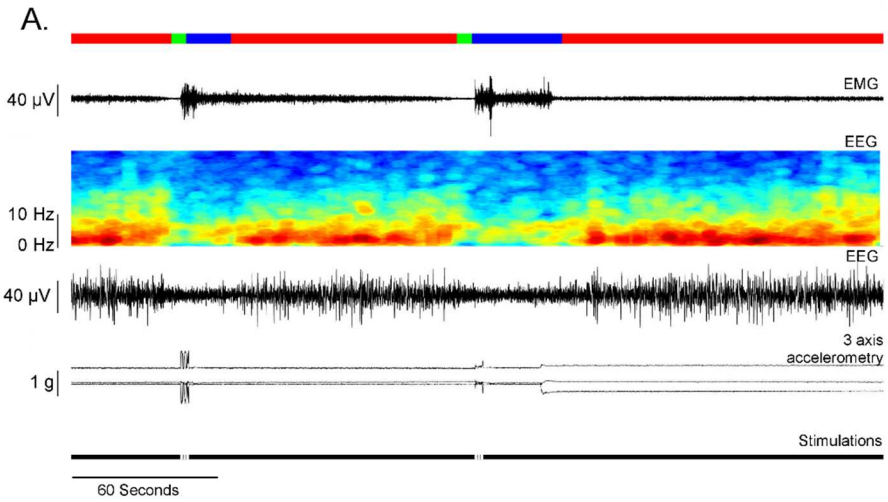

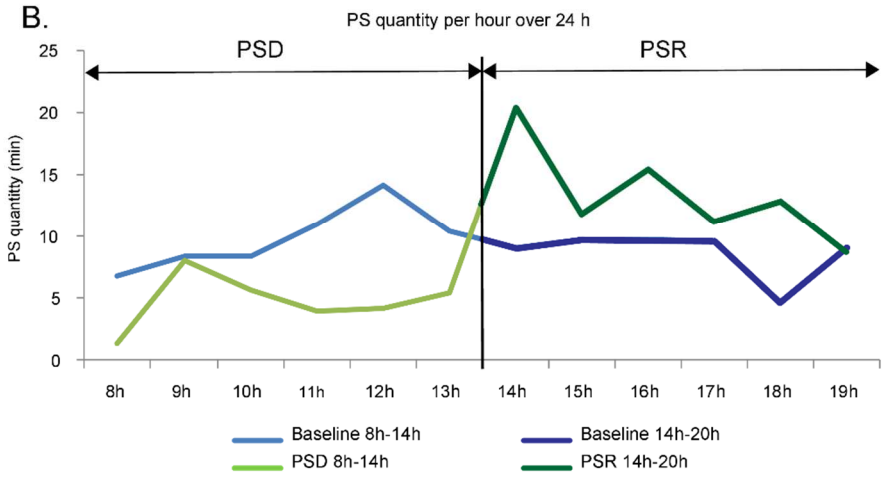

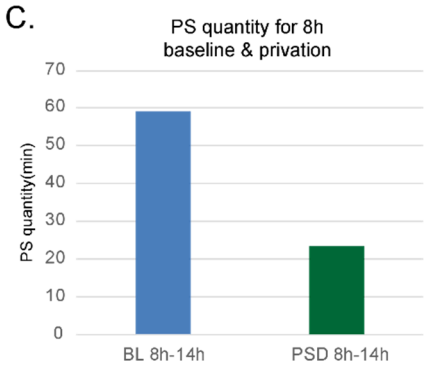

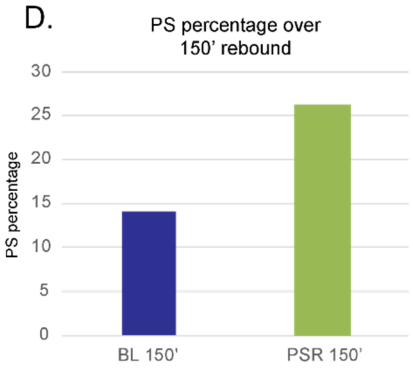

E.

PSD method	PSD Duration	Residual PS	PS Rebound over 150'
Gentle Handling with EEG/EMG Recordings (n = 20) Ravassard et al., 2015, Cereb. Cortex	4h	2.60 +/- 0.3% (vs. 9.5% in BL)	17.90 +/- 0.1%
APSD (n = 4) Unpublished data	6h	2.7 +/- 0,5% (vs. 12.3 +/-1.2% in BL)	24.6 +/- 2,3% (vs. 10.5 +/- 1.1% in BL)
ONEIROS (n=1)	6h	5% (vs. 16.6% in BL)	26.2% (vs. 14% in BL)

474

Fig. 11. Paradoxical Sleep deprivation efficiency. A. Hypnogram showing vigilance states (wake in blue, Slow wave sleep (SWS) in red, and Paradoxical Sleep (PS) in green), raw EMG signal, EEG time frequency and the associated raw EEG signal, and accelerometry. The bottom black bar shows when a stimulation was sent to awaken the animal (white bar). B. Percent time spent in PS per hour over the 12-hour baseline (in light blue 8h-14h and dark blue 14h-20h), PS deprivation period (from 8 to 14h in light green), and PS recovery period (from 14h to 20h in dark green). B. the histogram shows the mean quantity in minutes of PS during 6-hour baseline (left) compared to the remaining quantity of PS during PSD (right). C. The histogram illustrates the increase in PS after deprivation by showing the percentage of PS during 6 hours of baseline (left) compared to the 6 hours after the deprivation (right). D. the table compares the residual quantities of PS during PSD and PSR, during 4 hours of PS deprivation enforced via gentle handling (Ravassard et al., 2016), 6 hours of automated PS deprivation induced by a custom shaking device (Libourel et al., 2015), and ONEIROS PS deprivation.

3. Multiple parameters recorded in baseline condition with ONEIROS (logger version) in a pigeon

The electrophysiological and behavioral aspects of sleep recorded with ONEIROS in the pigeon were similar to those recorded in birds using other methods. Fig. 12. illustrates raw recordings with alternating periods of QW and AW, followed by SWS. The periods of AW were characterized by increased muscle activity and increased motion (visible on the accelerometry channels), and desynchronized EEG activity. The two peaks at 12 Hz and 24 Hz present on the power spectrum of AW (Fig. 12. A) resulted from head scratching. The periods of QW were characterized by low muscle activity (Fig. 13. B), comparatively small and infrequent changes in the accelerometry signal, generated by the birds' head movements, and desynchronized EEG activity. During SWS the EEG showed increased low frequency activity, when compared to all other states, increased Delta/Gamma ratio (Fig. 13. C) and the near absence of motion. Muscle tone usually remained at a level comparable to QW.

PS was characterized by EEG activation and behavioral signs of reduced muscle tone (e.g. head dropping as shown in the accelerometry recordings). As in other studies on pigeons and other avian species, the nuchal EMG rarely showed a reduction in activity, despite the behavioral signs of reduced tone. The number of eye movements increased during PS when compared to SWS. As previously described in pigeons and other birds (e.g. Dewasmes et al., 1985; Tobler and Borbély, 1988), eye movements included saccades, as well as faster oscillations (at 25-30 Hz). Unlike saccades which rarely occurred during SWS, the fast oscillations occurred during all sleep and waking states. They are thought to disperse oxygen and nutrients in the vitreous humor of the avian eye by moving a membrane (pecten) that protrudes inside the vitreous humor (Pettigrew et al., 1990).

Overall, the duration and timing of sleep bouts, as well as the amount of each state was typical for pigeons (Fig. 13. E). During the 12-h night, the bird spent 82.9% and 9.5% of the time in SWS and PS, respectively (Fig. 13. D).

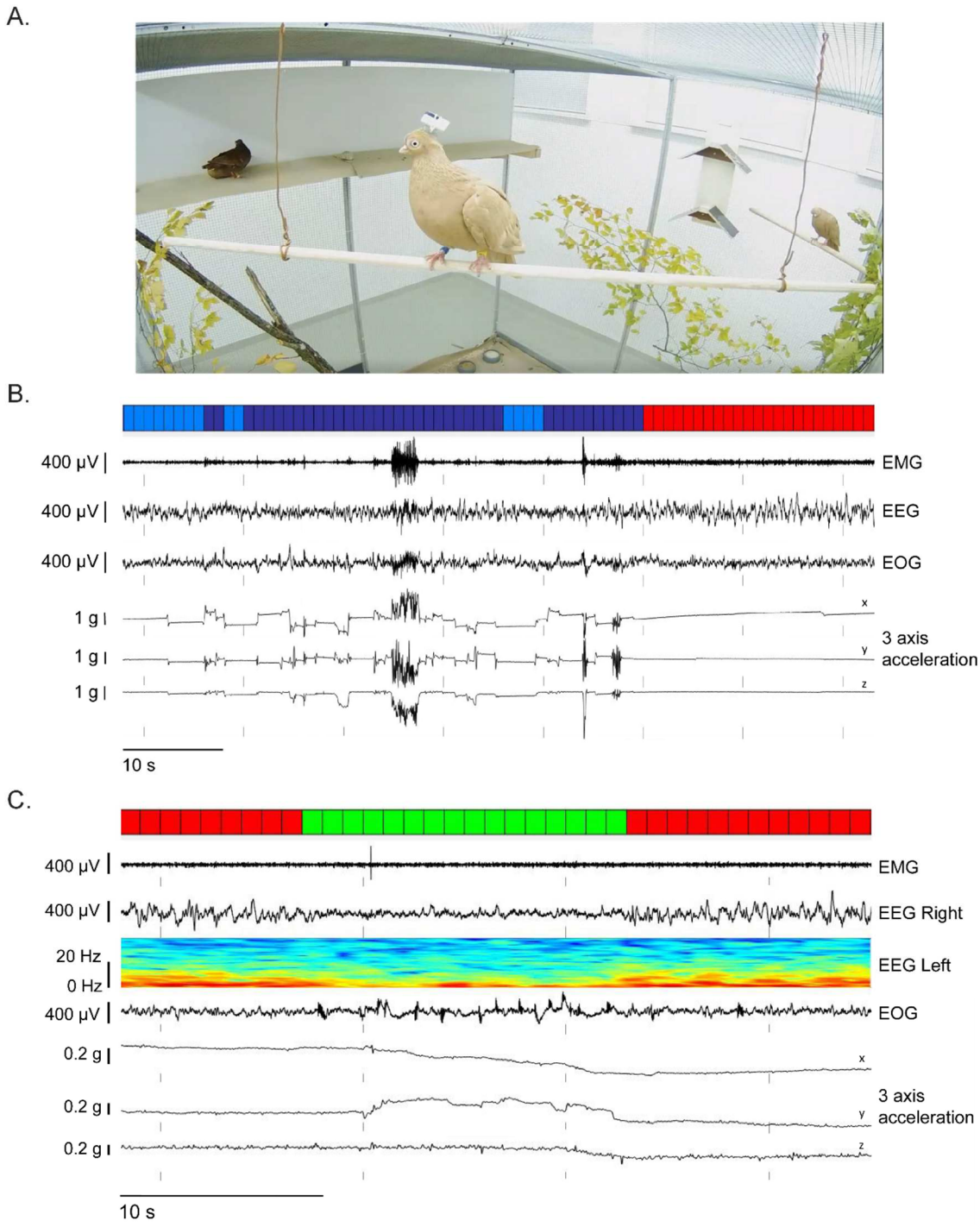

Fig. 12. Raw signals obtained with ONEIROS in logger mode from a pigeon during different vigilant states. A. Pigeon wearing ONEIROS (logger version) in the aviary during recording B. Raw signal illustrating the transition from wake to slow wave sleep (SWS). C. Raw signal illustrating one paradoxical sleep (PS) episode preceded and succeeded by SWS. From the top to the bottom; hypnogram illustrating the wake/sleep scoring (active wake in dark blue, quiet wake in light blue, SWS in red, and PS in green); EMG with a high pass filter (cutoff frequency 10Hz, order 2); right EEG; for B. only - time frequency representation of the left EEG; EOG; 3-axial accelerometry.

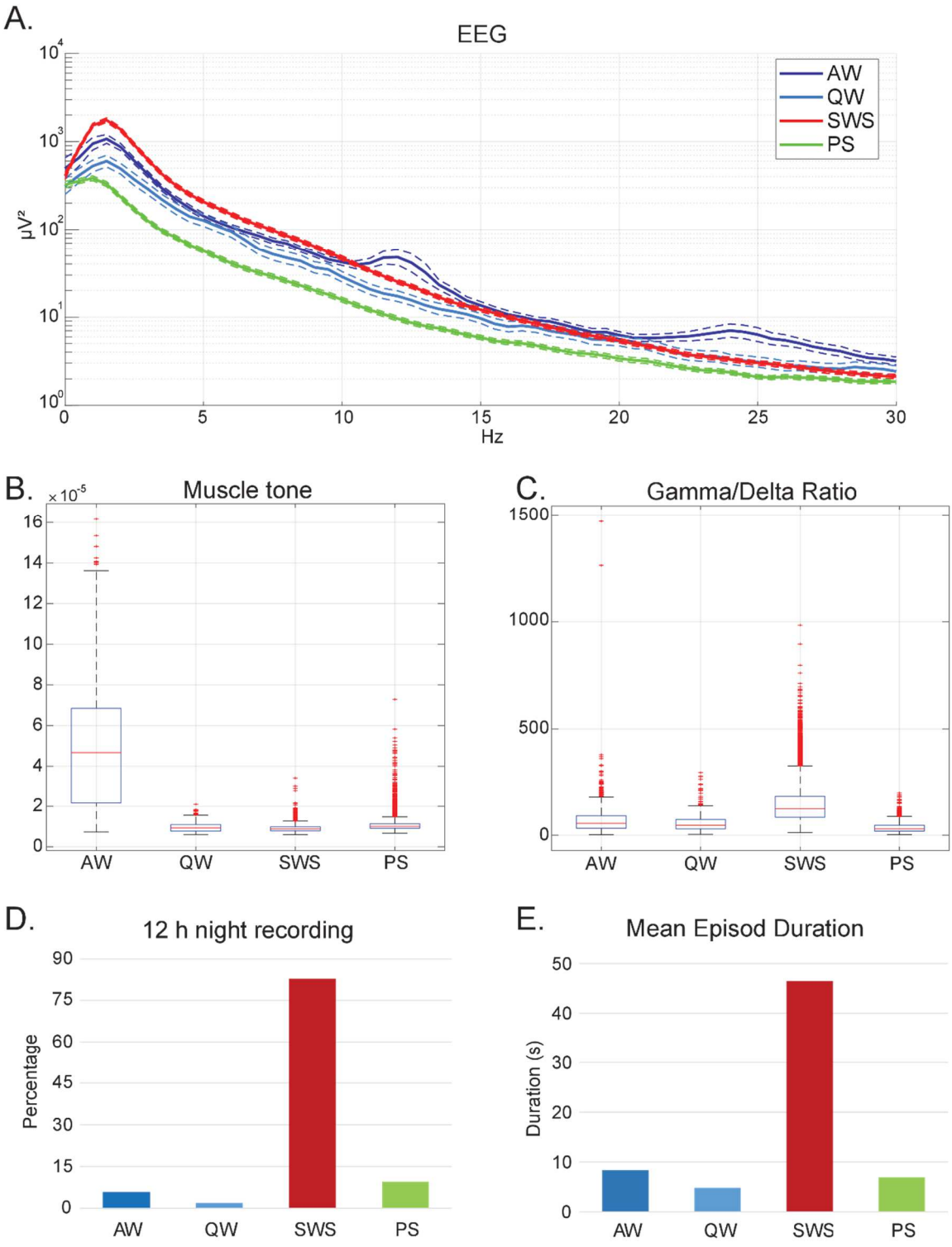

Fig. 13. Characteristics of wakefulness and sleep obtained from 12h night recordings of a pigeon with the ONEIROS logger. A. Power spectrum in each state computed for right EEG. B. Distribution of the muscle tone per epoch for each state. C. Distribution of the Delta/Gamma ratio for each state. D. Percentage of time spent in

each state during 12h night recordings. E. Mean episode duration for each state. AW – active wakefulness; QW – quiet wakefulness; SWS – slow wave sleep; PS – paradoxical sleep. Accelerometry axis direction: x – forward-backwards, y – lateral, z – vertical.

IV. DISCUSSION

1. Recording electrophysiology, behavior and temperature using a miniature instrument

One of the main reasons for developing ONEIROS was to combine in one small, light wireless device all of the electronics required to record multiple parameters related to sleep for long periods of time in small animals. Technically, the main constraints are size, weight, and autonomy. By coupling a frontend designed to record electrophysiology, an integrated digital accelerometer, a circuit to record temperature from multiple thermistors, and a low power microcontroller, we were able to build a system for studying sleep in small animals. Our recordings in baseline conditions in a rat, demonstrated that the size, weight, and autonomy of the system meet the requirements for recording sleep in the laboratory setting. Indeed, for the first time we were able to record without artefact in a freely moving animal most of the physiological and metabolic parameters that covary with sleep states (EEG, EMG, EOG, ECG, LFPs, and brain and body temperature). Moreover, we were also able to record the posture and the acceleration of the head via a 3 axis accelerometer, as well as ambient temperature. Our results and analysis demonstrate that an overall view of the classical features of sleep can be obtained with a single device. For example, the system can simultaneously record 10 electrophysiological channels at 256 Hz, three temperatures, and three acceleration channels at 64 Hz, for 35 hours with a 150 mAh; or 64 hours with 4 EEG, 1 temperature and 1 acceleration at 128Hz; an infinite number of other recording configurations are also possible. To our knowledge, in contrast to other commercial and/or published devices, ONEIROS is the only one that provides such flexibility in the configuration of the channels number and sampling rate, allowing users to completely customize data acquisition according to their needs.

In terms of limitation, while the system is small enough to be worn by rats, it is too large to be used on smaller animals such as mice. We estimate that the device is only suitable for animals over 100g. Future efforts should be directed toward reducing the size and weight of the device further, maybe with some compromises in term of capability and flexibility. Regarding the fields of application, although the system was designed for recording sleep, it could be used for other neuroscience applications. Behavioral tasks such as mazes, novel object recognition, and fear conditioning that require freely moving animals, might also benefit from the use of ONEIROS. Moreover, the device might be useful in studies using animal models of epilepsy wherein long-term recordings are needed to capture seizure related brain activity and behaviors.

2. Sleep deprivation with ONEIROS

For the first time a vibration motor integrated in a wireless recording device has been used to perform automated, real-time PS deprivation. Our results indicated that the stimulation was intense enough to awaken the

animal and thereby induce sleep deprivation. The system effectively reduced PS across a 6-hour period, and induced a homeostatic increase in PS following deprivation similar to that observed using other methods, such as gentle handling and shaking the floor of the animal's cage. However, the remaining quantity of PS during PSD was a bit higher compared to the other methods, likely because the stimulation was less intense compared to gentle stimulation or cage shaking. This also suggests that it might be difficult to awaken the animal with the device and settings used during longer term sleep deprivations. Possible solutions to this problem would be either to increase the duration of the stimulations (700ms in our experiments) or randomized the pattern of the stimulations. Another possibility would be to encapsulate the vibrating motor inside the dental cement, directly over the head of the animal.

3. Evaluation of the arousal thresholds with ONEIROS

In addition to the main parameters that characterized sleep (electrophysiology, posture, temperature), including its homeostatic regulation, arousal threshold is also an important feature of sleep. With ONEIROS, the intensity, occurrence, and duration of the vibrating motor stimulation can also be specified, allowing for the systematic assessment of arousal thresholds.

4. Recording sleep in semi natural environment with ONEIROS

By changing the wireless transmission stack to the logger stack, the device can be quickly transformed from a lab-based device to a logger suitable for recording sleep in the field. In this regard, ONEIROS does not need any additional systems to store the data (receiver, computer), as the signals are stored directly on an integrated SD card. In the logger configuration, sleep can be recorded in wild using methods previously employed with data loggers having fewer capabilities (Rattenborg et al., 2016). To demonstrate the feasibility of recording sleep in the field, we implanted a pigeon and recorded its vigilance states in an aviary where other birds were also housed. The instrumented bird displayed normal behavior including short flights in the 2 x 2 x 2 m aviary. Thus the system could be used in a completely natural environment, as previously done with a logger with fewer recording capabilities (Lesku et al., 2012; Rattenborg et al., 2016; Vyssotski et al., 2009). In comparison to this system, ONEIROS includes the capacity to record temperature, a useful parameter for evaluating the relationship between ambient temperature, body temperature, and sleep (SWS and PS) and hibernation or torpor under natural conditions. In addition, it can record more channels, which is necessary when recording sleep in a species for the first time. ONEIROS provides more sleep parameters combined in a single miniature device than other devices used for recording into the wild. Future improvements of ONEIROS will include a recording scheduler, in order to define specific recording periods. For example, this could be used to exclude the post-operative recovery period, and thereby extend the recording duration capability of the device. Moreover, we plan to develop waterproofing and other protections necessary for recording in the wild.

V. CONCLUSION

ONEIROS was developed to record multiple aspects of sleep (behavior, electrophysiology, metabolism) from animals in the lab and the wild. The goal was to provide researchers with a tool that overcomes the

limitations of existing wireless devices. The system provides high flexibility in terms of number of channels and sampling rate with low power consumption, allowing long-term recordings in small animals (from 100g). By wirelessly recording a rat under baseline conditions, performing a paradoxical sleep deprivation experiment in a rat, and logging data under semi-natural conditions in a pigeon, we demonstrated that ONEIROS is a useful tool for recording sleep under diverse conditions. For the first time EEG, EMG, EOG, ECG, LFPs, 3D acceleration, brain, body and ambient temperature recording, as well as homeostatic and arousal threshold experiments, can be conducted with the same system in the lab and in the wild on small animals. By facilitating comprehensive comparative and ecological studies of sleep, this device may lead to new perspectives regarding the evolution and functions of sleep.

VI. Acknowledgements

We are grateful for the financial support of the Université de Lyon through the Program 'Investissement d'Avenir' (ANR-1 1-IDEX-0007) and the CNRS interdisciplinary mission through the PEPS EXOMOD 2015-2016 (PHYLOREM project).

VII. References

Aserinsky, E., Kleitman, N., 1953. Regularly occurring periods of eye motility, and concomitant phenomena, during sleep. Science 118, 273–274.

Borbély, A.A., Neuhaus, H.U., 1979. Sleep-deprivation: Effects on sleep and EEG in the rat. J. Comp. Physiol. 133, 71–87. https://doi.org/10.1007/BF00663111

Campbell, S.S., Tobler, I., 1984. Animal sleep: a review of sleep duration across phylogeny. Neurosci Biobehav Rev 8, 269–300.

Corner, M.A., 1977. Sleep and the beginnings of behavior in the animal kingdom—Studies of ultradian motility cycles in early life. Progress in Neurobiology 8, 279–295.

Dement, W., 1960. The Effect of Dream Deprivation. Science 131, 1705–1707. https://doi.org/10.1126/science.131.3415.1705

Dewasmes, G., Cohen-Adad, F., Koubi, H., Le Maho, Y., 1985. Polygraphic and behavioral study of sleep in geese: existence of nuchal atonia during paradoxical sleep. Physiol. Behav. 35, 67–73.

Frank, M.G., Waldrop, R.H., Dumoulin, M., Aton, S., Boal, J.G., 2012. A Preliminary Analysis of Sleep-Like States in the Cuttlefish Sepia officinalis. PLoS ONE 7, e38125. https://doi.org/10.1371/journal.pone.0038125

Harrison, R.R., Fotowat, H., Chan, R., Kier, R.J., Olberg, R., Leonardo, A., Gabbiani, F., 2011. Wireless Neural/EMG Telemetry Systems for Small Freely Moving Animals. IEEE Transactions on Biomedical Circuits and Systems 5, 103–111. https://doi.org/10.1109/TBCAS.2011.2131140

Hawley, E.S., Hargreaves, E.L., Kubie, J.L., Rivard, B., Muller, R.U., 2002. Telemetry system for reliable recording of action potentials from freely moving rats. Hippocampus 12, 505–513. https://doi.org/10.1002/hipo.10040

Heller, H.C., Graf, R., Rautenberg, W., 1983. Circadian and arousal state influences on thermoregulation in the pigeon. Am. J. Physiol. 245, R321-328. https://doi.org/10.1152/ajpregu.1983.245.3.R321

Jouvet, M., Michel, F., Courjon, J., 1959. [On a stage of rapid cerebral electrical activity in the course of physiological sleep]. C. R. Seances Soc. Biol. Fil. 153, 1024–1028.

Klein, B.A., Olzsowy, K.M., Klein, A., Saunders, K.M., Seeley, T.D., 2008. Caste-dependent sleep of worker honey bees. Journal of Experimental Biology 211, 3028–3040. https://doi.org/10.1242/jeb.017426

Klein, M., Michel, F., Jouvet, M., 1964. [POLYGRAPHIC STUDY OF SLEEP IN BIRDS]. C. R. Seances Soc. Biol. Fil. 158, 99–103.

Lapray, D., Bergeler, J., Dupont, E., Thews, O., Luhmann, H.J., 2008. A novel miniature telemetric system for recording EEG activity in freely moving rats. Journal of Neuroscience Methods 168, 119–126. https://doi.org/10.1016/j.jneumeth.2007.09.029

Lesku, J.A., Meyer, L.C.R., Fuller, A., Maloney, S.K., Dell'Omo, G., Vyssotski, A.L., Rattenborg, N.C., 2011. Ostriches Sleep like Platypuses. PLoS ONE 6, e23203. https://doi.org/10.1371/journal.pone.0023203

642 Lesku, J.A., Rattenborg, N.C., Valcu, M., Vyssotski, A.L., Kuhn, S., Kuemmeth, F., Heidrich, W., Kempenaers,
643 B., 2012. Adaptive Sleep Loss in Polygynous Pectoral Sandpipers. Science 337, 1654–1658.
644 https://doi.org/10.1126/science.1220939
645 Libourel, P.-A., Corneyllie, A., Luppi, P.-H., Chouvet, G., Gervasoni, D., 2015. Unsupervised online classifier in
646 sleep scoring for sleep deprivation studies. Sleep 38, 815–828. https://doi.org/10.5665/sleep.4682
647 Libourel, P.-A., Herrel, A., 2016. Sleep in amphibians and reptiles: a review and a preliminary analysis of
648 evolutionary patterns: Sleep in amphibians and reptiles. Biological Reviews 91, 833–866.
649 https://doi.org/10.1111/brv.12197
650 Mohseni, P., Najafi, K., Eliades, S.J., Wang, X., 2005. Wireless Multichannel Biopotential Recording Using an
651 Integrated FM Telemetry Circuit. IEEE Transactions on Neural Systems and Rehabilitation Engineering
652 13, 263–271. https://doi.org/10.1109/TNSRE.2005.853625
653 Nath, R.D., Bedbrook, C.N., Abrams, M.J., Basinger, T., Bois, J.S., Prober, D.A., Sternberg, P.W., Gradinaru,
654 V., Goentoro, L., 2017. The Jellyfish Cassiopea Exhibits a Sleep-like State. Current Biology 27, 2984-
655 2990.e3. https://doi.org/10.1016/j.cub.2017.08.014
656 Omond, S., Ly, L.M.T., Beaton, R., Storm, J.J., Hale, M.W., Lesku, J.A., 2017. Inactivity Is Nycthemeral,
657 Endogenously Generated, Homeostatically Regulated, and Melatonin Modulated in a Free-Living
658 Platyhelminth Flatworm. Sleep 40. https://doi.org/10.1093/sleep/zsx124
659 Parmeggiani, P.L., 2003. Thermoregulation and sleep. Frontiers in Bioscience 8, s557–567.
660 Pettigrew, J.D., Wallman, J., Wildsoet, C.F., 1990. Saccadic oscillations facilitate ocular perfusion from the
661 avian pecten. Nature 343, 362–363. https://doi.org/10.1038/343362a0
662 Piéron, H., 1913. Le problème physiologique du sommeil. Masson.
663 Raizen, D.M., Zimmerman, J.E., Maycock, M.H., Ta, U.D., You, Y., Sundaram, M.V., Pack, A.I., 2008.
664 Lethargus is a Caenorhabditis elegans sleep-like state. Nature 451, 569–572.
665 https://doi.org/10.1038/nature06535
666 Rattenborg, N.C., de la Iglesia, H.O., Kempenaers, B., Lesku, J.A., Meerlo, P., Scriba, M.F., 2017. Sleep
667 research goes wild: new methods and approaches to investigate the ecology, evolution and functions of
668 sleep. Philosophical Transactions of the Royal Society B: Biological Sciences 372, 20160251.
669 https://doi.org/10.1098/rstb.2016.0251
670 Rattenborg, N.C., Lima, S.L., Amlaner, C.J., 1999. Half-awake to the risk of predation. Nature 397, 397–398.
671 https://doi.org/10.1038/17037
672 Rattenborg, N.C., Martinez-Gonzalez, D., Lesku, J.A., 2009. Avian sleep homeostasis: Convergent evolution of
673 complex brains, cognition and sleep functions in mammals and birds. Neuroscience & Biobehavioral
674 Reviews 33, 253–270. https://doi.org/10.1016/j.neubiorev.2008.08.010
675 Rattenborg, N.C., Voirin, B., Cruz, S.M., Tisdale, R., Dell'Omo, G., Lipp, H.-P., Wikelski, M., Vyssotski, A.L.,
676 2016. Evidence that birds sleep in mid-flight. Nature Communications 7, 12468.
677 https://doi.org/10.1038/ncomms12468
678 Rattenborg, N.C., Voirin, B., Vyssotski, A.L., Kays, R.W., Spoelstra, K., Kuemmeth, F., Heidrich, W., Wikelski,
679 M., 2008. Sleeping outside the box: electroencephalographic measures of sleep in sloths inhabiting a
680 rainforest. Biology Letters 4, 402–405. https://doi.org/10.1098/rsbl.2008.0203
681 Ravassard, P., Hamieh, A.M., Joseph, M.A., Fraize, N., Libourel, P.-A., Lebarillier, L., Arthaud, S., Meissirel,
682 C., Touret, M., Malleret, G., Salin, P.-A., 2016. REM Sleep-Dependent Bidirectional Regulation of
683 Hippocampal-Based Emotional Memory and LTP. Cerebral Cortex 26, 1488–1500.
684 https://doi.org/10.1093/cercor/bhu310
685 Rutz, C., Hays, G.C., 2009. New frontiers in biologging science. Biology Letters 5, 289–292.
686 https://doi.org/10.1098/rsbl.2009.0089
687 Scriba, M.F., Harmening, W.M., Mettke-Hofmann, C., Vyssotski, A.L., Roulin, A., Wagner, H., Rattenborg,
688 N.C., 2013. Evaluation of two minimally invasive techniques for electroencephalogram recording in
689 wild or freely behaving animals. Journal of Comparative Physiology A 199, 183–189.
690 https://doi.org/10.1007/s00359-012-0779-1
691 Shein-Idelson, M., Ondracek, J.M., Liaw, H.-P., Reiter, S., Laurent, G., 2016. Slow waves, sharp waves, ripples,
692 and REM in sleeping dragons. Science 352, 590–595. https://doi.org/10.1126/science.aaf3621
693 Siegel, J.M., 2008. Do all animals sleep? Trends in Neurosciences 31, 208–213.
694 https://doi.org/10.1016/j.tins.2008.02.001
695 Sławińska, U., Kasicki, S., 1998. The frequency of rat's hippocampal theta rhythm is related to the speed of
696 locomotion. Brain Res. 796, 327–331.
697 Snyder, F., Hobson, J.A., Morrison, D.F., Goldfrank, F., 1964. Changes in respiration, heart rate, and systolic
698 blood pressure in human sleep. J Appl Physiol 19, 417–422.
699 Sodagar, A.M., Perlin, G.E., Yao, Y., Najafi, K., Wise, K.D., 2009. An Implantable 64-Channel Wireless
700 Microsystem for Single-Unit Neural Recording. IEEE Journal of Solid-State Circuits 44, 2591–2604.
701 https://doi.org/10.1109/JSSC.2009.2023159

Tang, X., D. Sanford, L., 2002. Telemetric Recording of Sleep and Home Cage Activity in Mice. Sleep 25, 677–685. https://doi.org/10.1093/sleep/25.6.677

Tang, X., Orchard, S.M., Liu, X., Sanford, L.D., 2004. Effect of varying recording cable weight and flexibility on activity and sleep in mice. Sleep 27, 803–810.

Tobler, I., Borbély, A.A., 1988. Sleep and EEG spectra in the pigeon Columba livia under baseline conditions and after sleep deprivation. J. Comp. Physiol. 163, 729–738. https://doi.org/10.1007/BF00604050

Voirin, B., Scriba, M.F., Martinez-Gonzalez, D., Vyssotski, A.L., Wikelski, M., Rattenborg, N.C., 2014. Ecology and Neurophysiology of Sleep in Two Wild Sloth Species. Sleep 37, 753–761. https://doi.org/10.5665/sleep.3584

Vyssotski, A.L., 2005. Miniature Neurologgers for Flying Pigeons: Multichannel EEG and Action and Field Potentials in Combination With GPS Recording. Journal of Neurophysiology 95, 1263–1273. https://doi.org/10.1152/jn.00879.2005

Vyssotski, A.L., Dell'Omo, G., Dell'Ariccia, G., Abramchuk, A.N., Serkov, A.N., Latanov, A.V., Loizzo, A., Wolfer, D.P., Lipp, H.-P., 2009. EEG Responses to Visual Landmarks in Flying Pigeons. Current Biology 19, 1159–1166. https://doi.org/10.1016/j.cub.2009.05.070

Weiergräber, M., Henry, M., Hescheler, J., Smyth, N., Schneider, T., 2005. Electrocorticographic and deep intracerebral EEG recording in mice using a telemetry system. Brain Research Protocols 14, 154–164. https://doi.org/10.1016/j.brainresprot.2004.12.006

Yin, M., Borton, D.A., Komar, J., Agha, N., Lu, Y., Li, H., Laurens, J., Lang, Y., Li, Q., Bull, C., Larson, L., Rosler, D., Bezard, E., Courtine, G., Nurmikko, A.V., 2014. Wireless Neurosensor for Full-Spectrum Electrophysiology Recordings during Free Behavior. Neuron 84, 1170–1182. https://doi.org/10.1016/j.neuron.2014.11.010

Zayachkivsky, A., Lehmkuhle, M.J., Fisher, J.H., Ekstrand, J.J., Dudek, F.E., 2013. Recording EEG in immature rats with a novel miniature telemetry system. Journal of Neurophysiology 109, 900–911. https://doi.org/10.1152/jn.00593.2012

SUPPLEMENTARY VIDEO LEGENDS

Supplementary Video 1: the video illustrates the online paradoxical sleep deprivation on the rat. From the top to the bottom: the hypnogram (in red SWS, in green PS, in blue WK), the differential EMG, the EOG, the raw and time frequency representation of the parietal EEG. The video has been accelerated 2 times. In the top left corner a red rectangle appears when a stimulation was send.